How to Cite:
Moaeaa, M. S., & Al-Adilee, K. J. (2022). Preparation complexes Co(III), Ni(II), and Cu(II) with novel azo-Schiff base ligand (N, N, O) derived from 2- amino- 6- methoxy benzothiazole with spectral characterization, study biological activity as anti-cancer, anti-oxidant to complexes. *International Journal of Health Sciences*, *6*(S3), 10043–10067. https://doi.org/10.53730/ijhs.v6nS3.9480

Preparation complexes Co(III), Ni(II), and Cu(II) with novel azo-Schiff base ligand (N, N, O) derived from 2- amino- 6- methoxy benzothiazole with spectral characterization, study biological activity as anti-cancer, anti-oxidant to complexes

Mohammed Shaker Moaeaa
Graduate student at the University of Al-Qadisiyah / College of Science / Department of Chemistry
*Corresponding author email: mohamedshaker19891989@gmail.com

Khalid Jawad Al-Adilee
Teacher of the College of Sciences

***Abstract*---**The biological activity of the Co (III), Ni (II), and Cu (II) complexes of bidentate azo-Schiff bases derived from the 2-amino-6-methoxy Benzothiazole has been investigated. The azo-Schiff bases and their metal complexes were described using element analyses, magnetic moment measurements, spectroscopic (IR, electronic, 1H NMR, XRD), and thermogravimetric examinations. An octahedral geometry has been postulated for Co (III), Ni (II), and Cu (II) complexes. Coordinated water was established by thermal and infrared data from the metal complexes. The anti-cancer and anti-oxidant capabilities of Schiff bases and their metal complexes have been investigated.

***Keywords*---**benzothiazole, azo-schiff, anti-cancer, anti-oxidant, biological activity.

Introduction

Azo dyes can be obtained through diazonium and coupling reactions, where the first two steps are prepared to form the diazonium salt of the aromatic amines, which reacts quickly with nitrous acid (HNO2) prepared immediately from the reaction of sodium nitrite (NaNO2) with concentrated hydrochloric acid (HCl) at a

temperature ranging from 5 -0 oC due to the instability of diazonium salt at high temperatures(Benkhaya et al. 2020). The second step is represented by pairing the diazonium salt prepared in the first step with the aromatic compound. Compared to simple aromatic compounds, these azo dye compounds produce a wide range of colors throughout the visible spectrum, where heterocyclic azo dyes generate an important color coating effect different colors can be produced by changing the functional groups incorporated into the azo molecule. Furthermore, these pigments are more stable and have greater resistance to light degradation over time than other dye molecules. Much research into azo compounds has been based on heterocyclic systems and their derivatives, such as benzothiazoles, thiophenes, thiazoles, and pyrazoles, due to their potential applications in a number of diverse fields. One area, in particular, involves the design of biologically active molecules for chemotherapy(Benkhaya et al. 2020; Harisha et al. 2017; Mallikarjuna and Keshavayya 2020).

The azo compounds that contain a heterogeneous ring have been of great interest to researchers because of their biological, industrial, and analytical applications. They have different applications in the fields of analytical chemistry, where they were used as guides and in manufacturing thin films. Such as antioxidant, antimicrobial, antineoplastic, antidiabetic, and antiviral(Mohammadi et al. 2015). In addition to its active role in the field of industry, it is used in the manufacture of cosmetics, food coloring, plastics, optical switches, optical data storage, non-linear optics, liquid crystal displays, and photovoltaic devices(Yadav et al. 2011). It is a class of heterocyclic sulfur-containing rings that includes a benzene ring incorporated into a thiazole ring. The benzothiazole ring system was initially found in many marines and terrestrial natural compounds(El-Ghamry et al. 2018; Maliyappa et al. 2019).

A series of novel 2-aminobenzothiazole derivatives were synthesized and evaluated for anti-inflammatory activity. The labeled compounds were synthesized from the aromatic amines substituted through the intermediate oxidation of 1-phenylthiourea by bromine water in an acidic medium. The purity of the prepared compounds was judged by C and H analysis. N and the structure were analyzed based on IR data, 1HNMR, and mass spectrometry. The new compounds' anti-inflammatory activities were determined by carrageenan-induced rat paw edema using diclofenac sodium as a standard. Among the compounds tested, three were Bt2 (5-chloro-1,3-benzothiazole-2-amine), Bt(6-methoxy-1,3-benzothiazole-2-amine), and Bt7 (6-methoxy-1,3 - benzothiazole-2-amine) is the most active compound in this series when compared to diclofenac sodium. In the SAR study, the phenyl ring was substituted for chloro at position 5, and the methoxy substitution at 4 and 6 in the benzothiazole ring system showed better antagonistic activity(Prakash et al. 2021).

Experimental Part
Chemicals and solvents

Amino-6-methoxy Benzothiazole, Sodium nitrite (NaNO2), HCl, and other chemicals used in this study are of pure quality (BDHA drich). 3-Amino phenol, 4-Dimethyl benzaldehyde, sodium hydroxide, ethanol, Glacial Acetic acid,

dimethylsulphoxide (DMSO), CoCl2.6H2O, NiCl2.6H2O, CuCl2. 6H2O and distilled water.

Physical measurements

The element analyzer EA 300 (CHNS) was used to determine ligand (HL) elemental microanalyses. The 1H and 13C NMR spectra were obtained with a Bruker 400 MHZ spectrometer, DMSO-d6 as the solvent, and TMS as the internal reference. On a T80-PG double beam (UV-Vis) spectrophotometer, the electronic spectra were obtained in absolute ethanol using a quartz cuvette with a 1 cm path length of 200–1100 nm. The mass spectra of ligands (BIAB) were recorded using a Shimadzu Agilent Technologies 5973C mass spectrometer (70 eV). X-ray diffraction (XRD) measurements were carried out using a Bestec Aluminium anode from Germany. X-ray diffractometer using (Cu K) radiation in the 20–80 range (14 1.5418A) FT-IR spectra were recorded using a Shimadzu 8400 S (KBr disks, 4000–400 cm1). Thermal analysis (TGA-DTA) was performed in a nitrogen environment using PL-TG equipment at temperatures ranging from 25 to 900 oC at a heating rate of 10 C min1. A scanning electron microscope is used to capture the images (FE-SEM). MIRA3 TESCAN The analysis was carried out using the Stuart instrument, which SMP has produced. The substance's melting point or decomposition temperature is noted. Ligand, capillary tube Philips PW 9421 pH meter has been used to take the readings. The chemical was synthesized using PerkinElmer Chem Bio Draw software, then optimized using PerkinElmer ChemBio3D software.

Synthesis of novel azo-Schiff base ligand (H L)
Benzothiazole azo ligand preparation

- Preparation of Schiff base
  The ligand (HL) was prepared based on what was prepared in our laboratory by Al-Adly and his group with some modifications to the method of work; Schiff base was prepared through a condensation reaction between the compound 4-Dimethylamine benzaldehyde and its molar equivalent (1:2) of the compound 3-aminophenol, like 1.2 g (0.01 mol) of 4-dimethylamine benzaldehyde was dissolved in 40 ml of absolute ethanol and mixed with a solution of 1.2 g (0.01 mol) of 3-aminophenol dissolved in 30 ml of the same mentioned solvent. Four drops of glacial acetic acid were added as a catalyst, followed by heating the mixture for (10-12) hours; the solution was left to cool and then poured over ice pieces of distilled water where pale-yellow crystals appeared, filtered, dried, and returned Crystallized with hot ethanol to obtain a base lip(Jaber et al. 2021).(Al-adilee and Hessoon 2019)
- Preparation of azo ligand - Schiff base (HL.)
  Dissolve 1.8 g (0.01 mol) of 2-amino-6-methoxybenzothiazole was dissolved in a mixture consisting of 5 ml of concentrated hydrochloric acid and 35 ml of distilled water, then the mixture was cooled to a temperature (0-5) oC, and a solution of 0.75 was added Gram (0.01 mol) of sodium nitrite (NaNO2) dissolved in 25 ml of distilled water-cooled to (0-4) drop by drop with continuous stirring, taking into account that the temperature does not rise above (5) oC. Leave the solution to settle for this diazonium solution was added dropwise and with continuous stirring to a solution of 2.13 g (0.01 mol)

of Schiff base prepared in paragraph (2-3-1-a) of this chapter and dissolved in a mixture consisting of (40) ml of alcohol) Pure ethyl ester and 10 ml of 10% sodium hydroxide solution and 5 ml of potassium sulfate solution 10%) it was noticed that the solution was colored in dark red(Al-Adilee and Shaimaa 2017). The mixture was stirred for one hour at a temperature (5-0) oC, filtered the solution, and washed the precipitate (purple crystals). light with distilled water several times, it was recrystallized using ethanol solution. The precipitate was dried using an electric furnace at a temperature of 50 oC for a few hours, and it was measured Ab the percentage of the prepared product and its melting point. Scheme (1) shows the denitrification processes and coupling to form the azo ligand - Schiff base (HL).

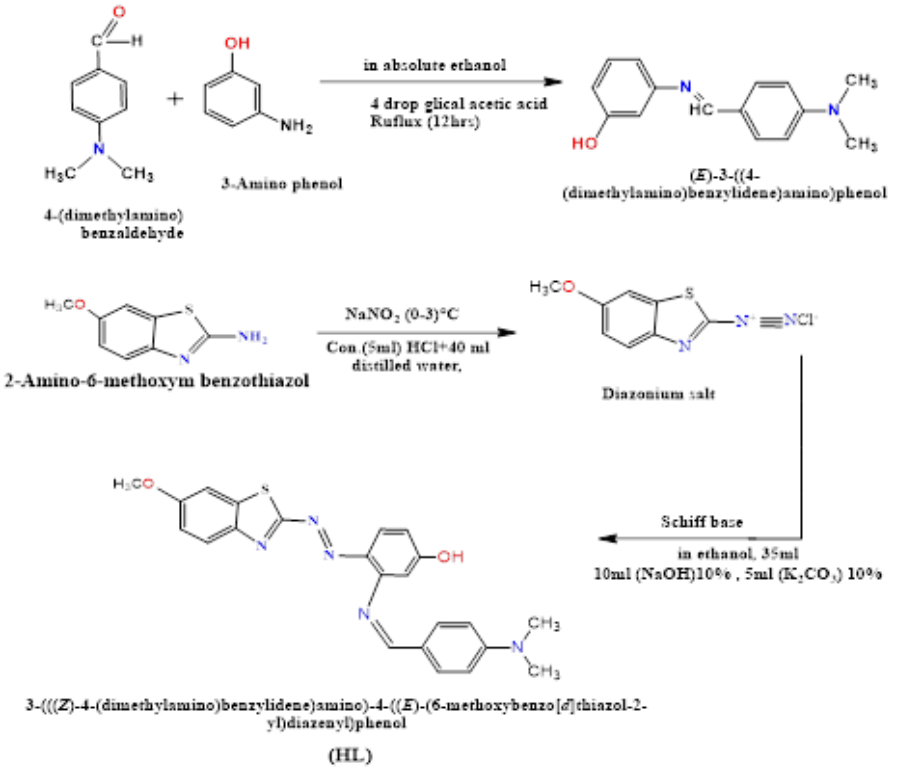

Scheme 1. Synthesis of novel azo-Schiff base ligand (HL)

Synthesis of the complexes

Complexes of ions of metal salts of Cobalt (III), nickel (II), and copper (II) with a molar ratio of [1:2] [M: L] were prepared by slowly adding the required weight for each ligand (0.001) mole of the prepared ligand dissolved in 25 ml of pure and absolute ethanol solvent and gradually stirring to the metal solution (0.0005) mol of the metal chlorides under study dissolved in 25 ml of the buffer solution at 60° C for 30 minutes with constant stirring The dark colors were left in the solutions for 24 hours to complete the sedimentation process, after which the sediments were filtered and washed several times with non-ionic water and then with a small

amount of ethanol solvent to remove unreacted organic matter, followed by recrystallization with absolute ethanol.

Results and Discussion

Characterization of azo dye ligand (HL) and its metal complexes

The synthesized compounds were stable in air and moisture at room temperature. They were water-insoluble. Dimethyl sulfoxide, methanol, ethanol, and dimethylformamide are all soluble in Dimethyl sulfoxide (DMF). The analytical results of the complexes matched the stoichiometry expected(Al-Adilee and Hesson 2015).

Mole ratio method

With 100% ethanol as the solvent, the metal: ligand [M: L] ratio was computed using the mole ratio method at different maximum values for each complex. UV–VIS spectrophotometry was used to analyze the composition of metal complexes at constant metal ion concentrations and wavelengths (max) and increasing ligand solution volume (0.25 ml each, adding up to 3.5 ml). Metal complex solutions with increasing color intensity and color stability at the point of contact are significant markers of metal complex production at the typical ratio. The results showed that the ligand reacted with metal ions in a [2:1] metal to ligand [M: L] mole ratio, which is consistent with our prior findings(Waheeb et al. 2022).

Table 1
Physical properties and element analysis for novel azo-Schiff base ligand (HL) their metal complexes, and the molar ratios added from the ligand and metals

Compound	Color	M.p °C	λ_{max}	Molecular formula (Mol. Wt)	Yield (%)	Found (Calc.) %					Molar conductivity $S.cm^2 mol^{-1}$
						C %	H %	N %	S%	M %	
(HL.) ligand	light yellow	126	425	C_{23} H_{21} N_5 O_2 S (431.51)	86	63.96 (64.36)	4.86 (4.88)	7.43 (7.93)	16.23 (16.58)	--	---
$[Co(HL)_2]Cl_3.H_2O$	light green	121	607	$C_{46}H_{44}$ $N_{10}Ni$ O_5 S_2 Cl_3 (1046.96)	83	52.72 (53.22)	4.20 (4.32)	13.38 (13.78)	6.12 (6.57)	5.62 (5.82)	75.3
$[Ni(HL)_2]Cl_2.H_2O$	greenish purple	170	595	$C_{46}H_{44}$ $N_{10}Cu$ O_5 S_2 Cl_2 (1010.63)	82	54.61 (55.11)	4.35 (4.43)	13.86 (14.36)	6.34 (6.64)	5.80 (6.05)	80.65
$[Cu(HL)_2]Cl_2.H_2O$	light olive	182	610	$C_{46}H_{44}$ $N_{10}Zn$	76	54.35 (54.6	4.33 (4.41)	13.79(14	6.31 (6.6	6.25	77.45

				O_5 S_2 Cl_2 (1015.48)		5)		.24)	6)	(6.55)	

Molar conductivity

The conductivity values of the metal complexes with the ligand (HL) indicated that they all have ionic character; Table (1) shows the molar conductance high values for the complexes cobalt (III), nickel (II), and copper (II) complexes with the ligand (HL) increased with this. It is evidence of the presence of the ionic character in it depending on the presence of the chloride ion outside the coordination sphere as a companion ion. When adding an aqueous solution of silver nitrate (AgNO3) to the solutions of the complexes mentioned above, it was observed that a white precipitate formed, which shows us the presence of chloride ions located outside the sphere Consistency). This agrees with the results obtained in proposing the structural and spatial shapes of the studied metal complexes(Kyhoiesh and Al-Adilee 2021).

H NMR studies
H- NMR spectroscopy of the ligand azo-Schiff base (HL)

The ligand (HL) was diagnosed using 1H-NMR proton spectroscopy using dimethyl sulfur dioxide DMSO-d6 as a solvent, and TMS (TMS) was used as a standard reference as mentioned in the literature. The -NMR of the ligand has multiple beams at chemical displacement δ= 3.02-3.06 ppm and it belongs to the protons of the methyl group ((–CH3) in position (30,31), where it showed a single beam at chemical displacement δ= 3.64-3.82 ppm which is back to the protons of the group The methyl (–CH3) at position (11) also showed two bands at chemical displacement δ = 6.56-6.80 ppm belonging to the aromatic ring protons at positions (24,25,27,28) and also appeared multiple at chemical displacement δ = 7.12-7.28 ppm It goes back to the aromatic ring protons at the sites (15, 16, 18), as well as a single beam appeared at the chemical displacement δ = 7.69-7.74 ppm and it goes back to the aromatic ring protons at the sites (4,5,7) while the single beam at the chemical displacement δ = 8.79-8.85ppm It belongs to the proton of the azomethine group (-N=CH) at the position (22), As for the single beam at chemical displacement δ = 9.33-9.39 ppm belonging to the proton of the terminal hydroxyl group (OH) at position (20), while the spectrum showed a beam at chemical displacement δ = 2.49 ppm belonging to the protons of the solvent DMSO-d6 Figure (1) shows the proton nuclear magnetic resonance spectrum of the ligand (HL).

Table 2
1H-NMR spectrum of ligand (HL) and nickel (II) complex

Ligand (HL)d, ppm (Hatom, peak, assignment)	J-J coupling	Ni(II)-complex d, ppm (H atom, peak, assignment)	J-J coupling
2.49 (DMSO-d_6)	3.47	2.50 (DMSO-d_6)	1.00
3.02-3.06 (6H,s,30,31)	6.17	3.01 (6H,s,30,31)	1.27

3.64-3.82 (3H,s,11)	2.93	3.94 (3H,s,11)	0.05
6.56-6.80 (4H,d,24,25,27,28)	4.35	6.54-7.21 (4H,d,24,25,27,28)	0.20
7.12-7.28 (3H,m,15,16,18)	4.20	7.38-7.5 (3H,m,15,16,18)	0.16
7.69-7.74 (3H,s,4,5,7)	2.82	7.88-7.94 (3H,s,4,5,7)	0.42
8.79-8.85 (1H,s,22)	0.34	8.40 (1H,s,22)	0.67
9.33-9.39 (1H,s,20)	0.99	9.11 (1H,s,20)	0.26

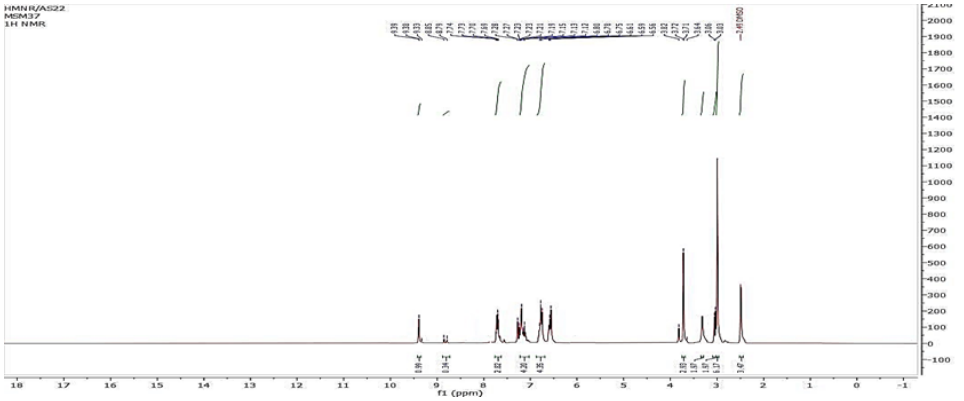

Figure 1. 1H-NMR spectrum of the ligand (HL.)

NMR proton spectrum of the nickel (II) complex: - [Ni (HL)2] Cl2.H2O

The proton 1H-NMR spectrum of the nickel complex showed a single beam at the chemical displacement δ=3.01 ppm belonging to the protons of the methyl molecule (–CH3) at the position (30,31), and also a single beam appeared at the chemical displacement δ= 3.94 ppm belonging to the protons of the methyl molecule (–CH3). –CH3) at position (11), and also a binary band appeared at chemical displacement δ = 6.54-7.21 ppm, Which belongs to the aromatic ring protons at positions (24,25,27,28), while the multiple beams at chemical displacement δ = 7.38- 7.5 ppm that goes back to the aromatic ring protons at sites (15, 16, 18), and a single beam appeared at the chemical displacement δ = 7.88-7.94 ppm belongs to the aromatic ring protons at sites (4,5,7), either The single beam at the chemical displacement δ = 8.40 ppm belongs to the proton of the azomethine group -N = CH) at the position (22), while the spectrum showed a single beam at the chemical displacement δ = 2.49 ppm belonging to the protons of the hydroxyl group at the site (20), in When the spectrum showed a single band at chemical displacement δ = 2.50 ppm belonging to the protons of the solvent DMSO-d6. Figure (2) shows the NMR spectrum of the nickel (II) complex.

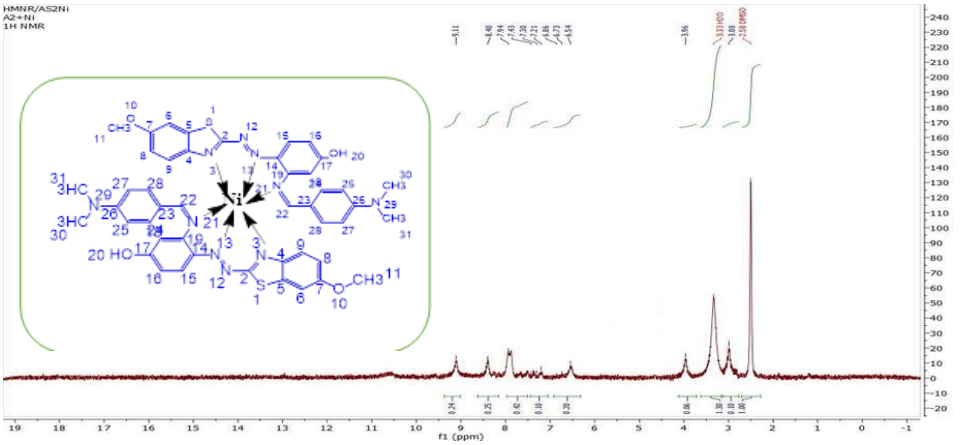

Figure 2. 1H-NMR spectrum of the nickel (II) complex [Ni (HL)2] Cl2.H2O

Infrared spectra studies

- Infrared spectrum ranged between (1700-4000) cm-1
  The infrared spectrum of Ligand (HL) gave a medium-intensity absorption band at a frequency of (3387) cm - attributed to the stretchy vibrations of the hydroxyl group (OH). This band did not undergo a noticeable change in the metallic complexes of Ligand (HL), indicating that it did not participate in the bonding(Khalid 2018; Prajapati et al. 2014).
- Infrared spectrum ranged between (400-1700) cm-1
  This region is one of the important regions in the interpretation of the infrared spectrum of metal complexes, as it includes many or most of the absorption bands that belong to the active groups in the spectra of the ligand and its metal complexes, including groups (C = N), (N = N), (C = C) and others. Of the other effective aggregates, in addition to the vibrations that belong to the (M-N) (metal-nitrogen) bond. By comparing the spectra of the metal complexes under study in this region of the spectrum with the spectra belonging to the free ligand, it was observed that the bands shifted, whether toward lower or lower frequencies. Higher frequencies, in addition to the emergence of new bands that were not present in the spectra of the ligands under study, indicate synergy. We will deal in detail with the ligand bands that were affected in coordination with the metal ions under study, where the infrared spectrum of the ligand (HL) gave medium intensity absorption bands at frequency 1640 (cm-1) belonging to the (C=N) bond in the benzothiazole ring of the ligand (HL) The spectra of the metal complexes showed a noticeable change in the position and intensity of these bands. This discrepancy and difference are due to the participation of the non-acoustic electronic double of the nitrogen atom of the benzothiazole ring coordinated with the metal ions under study. The spectra of the studied ligand gave several absorption bands within the range (1600-1200) cm-1 due to the vibrations of the υ (C - C) and υ (N = N) and (C = C), (C - S) and (C - S) bonds. O) in the spectra of the complexes of these beams(Al-Adely 2012). In the spectra of the complexes, it was noted that the beams had suffered changes in shape, location, and intensity and that the reason for the redshift of these beams is the occurrence of coordination between the metal ion and the nitrogen atom of the azo group

far from the benzothiazole ring by giving it a free electron pair, and this is what was indicated. According to several previous studies, the spectra of the ligand gave an absorption band at a frequency of 1436 cm-1 that was attributed to the vibration frequencies of the bond (-N=N-) υ that was attributed to the ligand (HL). A noticeable change in the intensity, shape, and location in the spectra of the metal complexes indicates the involvement of the electron pair belonging to the azo bridge group's nitrogen atom in the coordination process with the metal ions under study to form the metal complexes. The spectra of the free ligand also gave bands at frequency 1277 cm-1. It goes back to the frequency of the (C-S) bond of the benzothiazole ligand ring (HL). Also, the spectra of the metal complexes gave frequencies for new bands that were not present in the spectrum of the free ligand, as they belong to the metal-nitrogen (M-N) bonds. Thus, the infrared spectra indicate that the ligand (HL) behaves as three-tooth ligands through the coordination process. The coordination is through the benzothiazole ring's nitrogen atom with the azo bridge group's nitrogen atom far from the benzothiazole ring. Hence, the third binding site is through the nitrogen atom of the azomethine group to give two pentagonal rings that increase the stability of the formed metal complexes. The many changes mentioned and illustrated in Table (3) and Figure (3) is evidence added to the previous evidence mentioned about the occurrence of the process of coordination between the ligand (HL) and the metal ions under study to form metal complexes(Kyhoiesh and Al-Adilee 2022).

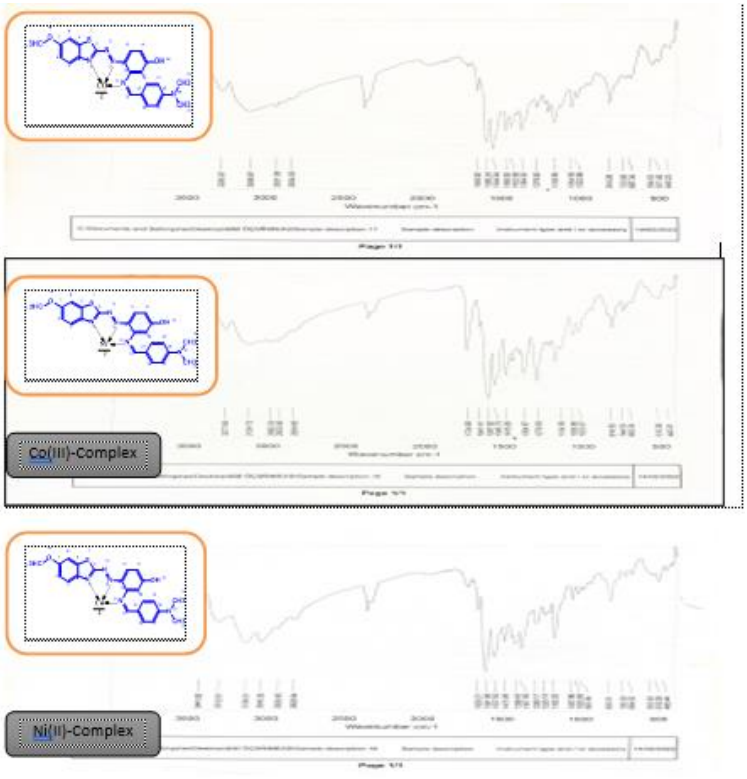

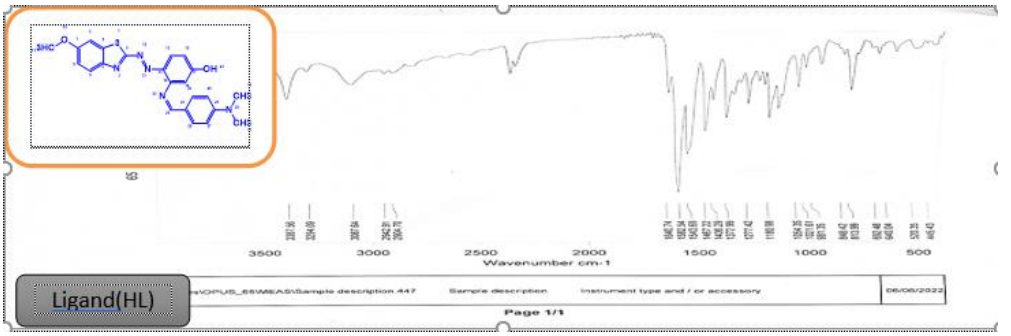

Figure 3. FT-IR spectrum of the ligand (HL) and its metal complexes.

Table 3
Infrared spectra frequencies (cm-1) for the azo ligand - Schiff base (HL) and its metal complexes

Group	Ligand (HL.)	Co(II) Complex	Ni(II) Complex	Cu(II) Complex
υ- OH	3387 m.br	3277m.br	3285m.br	3312m.br
υ - N-$(CH3)_2$	2942w	2933m	2931m	2929w
υ-(C=N) Ben.Thio	1582s	1587s	1586s	1591s
υ- (C=N) Schiff	1640m	1647w	1650m	1650m
υ- (N=N)	1436m	1410w	1432m	1399m
υ- (C=C)Ph	1543s	1546m	1544s	1537m
υ-(C-S)Thia	1277m	1279m	1276s	1280m
υ-(C-N)Thia	1180s	1134m	1159s	1163m
υ-(C-O)	1372m	1367m	1364s	1367m
υ-(M-N)	……	515m	554s	553 w

S=strong, m=medium, w=weak, br=broad

Electronic spectra studies
Electronic spectra of free ligand (HL)

The free ligand (HL) spectrum found three peaks, the first absorbing at 425 nm (23584.9) cm-1, returning to the (n-π*) transition, and the second returning to the electronic transition (π→π*) at 295 nm (33898) cm-1. For the azo groups (N=N) and (C=N). The third peak arose at a frequency of 250 nm (40000) cm-1, which was determined by the electron transfer (π→π*) of the (C=C) bond between the benzothiazole ring and the aromatic ring. It provided the cobalt (III) complex's UV-visible spectrum. There are three absorption peaks. The first three peaks at 607 nm (16474) cm-1, 442 nm (22624) cm-1, and 250 nm (40,000) cm-1 are produced by the 1A2g →1T2g(F) (υ1), 1A2g →1T1g(F (υ2), 1A2g →1T1g(p) (υ3) electronic transitions and its postulated regular octahedral geometry, as well as its hybridization d2sp3. The electronic spectra of the nickel (II) complex found three absorption peaks, the first at 968 nm (10330) cm-1, the second at 595 nm

(16806) cm-1, and the third at 383 nm (26109) cm-1, and is associated with the electronic transmissions 3A2g3 T2g(F)(□1), 3A2g3 T1g(F) (□2), and 3A2g3 3T1g(p)(□3). The geometry of the regular octahedral complex and its hybridization was sp3d2. The electronic spectrum of the copper complex gave a broad mid-intensity absorption peak at a frequency of 610 nm (16393) cm-1. The reason for the width of the peak indicates three electronic transitions: 2B1g→ 2A1g (□1), 2B1g→ 2B2g (□2), and 2B1g→ 2E2g (□3). The same in energy showed one broad absorption band due to the electron transition 2B1g → 2Eg, due to the effect of Jan Teller in the width of this peak. And the proposed geometry is octahedral with deformed deformation, and the deformation type is compressed (Z-in) or dragged (Z-out). The most common possibility is (Z-out) and its sp3d2 hybridization(Alshamsi et al. 2021).

Table 4
Electron transfer spectra of the azo ligand - schiff base (hl) and its complexes

Compounds	λ_{max}(nm)	Absorption Bands cm^{-1}	Transitions	μ_{eff} BM.	Geometry	Hybridization
Ligand=HL	425	23384	n—π*	-	-	-
	295	33898	π —π*			
	250	40000	π —π*			
$[Co(HL)_2]Cl_3.H_2O$	607	16474	$^1A_2g \rightarrow {}^1T_2g_{(F)}(\upsilon_1)$	Dia	Octahedral (Regular)	$d^2 sp^3$ (Low spin)
	442	22624	$^1A_2g \rightarrow {}^1T_1g_{(F)}(\upsilon_2)$			
	250	40000	$^1A_2g \rightarrow {}^1T_1g_{(p)}(\upsilon_3)$			
$[Ni(HL)_2]Cl_2.H_2O$	968	10330	$^3A_2g \rightarrow {}^3T_2g_{(F)}(\upsilon_1)$	2.81	Octahedral (Distorted) (Z-in or Z-out)	Sp^3d^2 (high spin)
	595	16806	$^3A_2g \rightarrow {}^3T_1g_{(F)}(\upsilon_2)$			
	383	26109	$^3A_2g \rightarrow {}^3T_1g_{(p)}(\upsilon_3)$			
$[Cu(HL)_2]Cl_2.H_2O$	512	19230.8	$^2B_1g \rightarrow {}^2Eg$	1.78	Octahedral (Regular)	Sp^3d^2

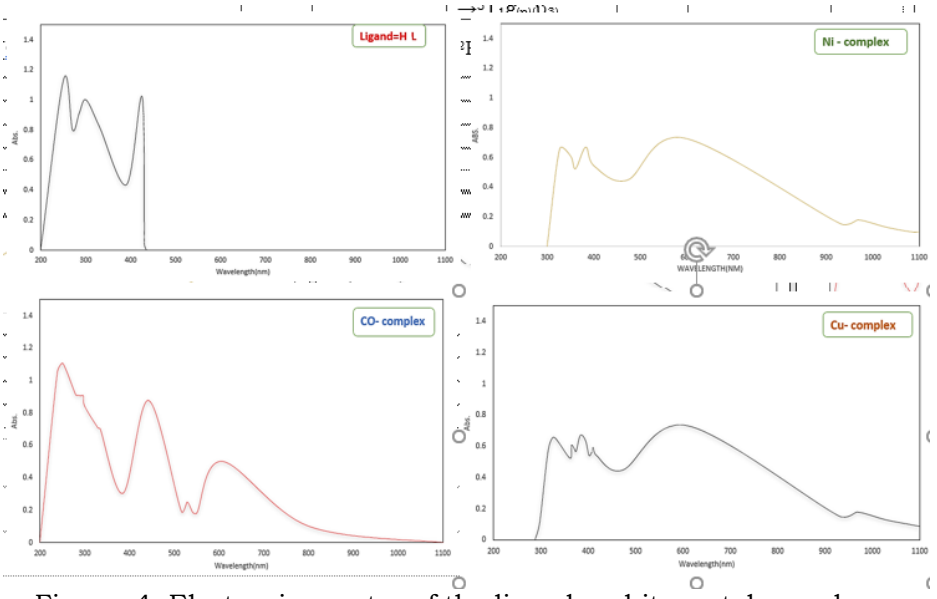

Figure. 4. Electronic spectra of the ligand and its metal complexes

Magnetic susceptibility studies

The magnetic susceptibility of the synthesized complexes was recorded at room temperature. The value of the effective magnetic moment for the cobalt (III) complex showed diamagnetic properties (t2g6 eg0) as the twist is low and the proposed shape of the prepared complexes is regular octahedral with d2sp3 hybridization of the central atom. It is considered one of the inner orbital complexes. The nickel (II) complex of ligand (HL) is 2.81 BM = effμ, which indicates the presence of paramagnetic properties. This is the presence of two single electrons for the regular octahedral complex (t2g6 eg2). The hybridization of the central atom is sp3d2, meaning that it is considered one of the complexities of the outer orbital, which is agreed upon in the literature. The magnetic susceptibility of the copper (II) complex gave paramagnetic properties where it was 1.78 = effμ BM. The reason for this is the presence of one single electron. The proposed shape of the complex is a distorted octahedron that may be (Z-in or Z-out) of the order (t2g6 eg3) and hybridization sp3d2. It is an exogenous orbital complex (Bai et al. 2011). This result is given in Table (4).

Field-emission scanning electron microscope analysis (FE-SEM)

The surface properties of the azo-ligand Schiff base (HL) particles and their metal complexes with the metal ions under study, namely couplet (III), nickel (II), and copper (II), in terms of the crystalline shape of the particles and aggregates, were conducted by using scanning electron microscope technique with a cross-sectional distance of 5.9 m, and Magnification power K X Mag = 50.00 and through the FESEM analysis image of the ligand (HL) where it became clear to us that its shape is heterogeneous crystals and the average size has reached 86.4 nm. The particle size of the Co (III) complex is 59 nm. At the same time, FESEM analysis of the Ni (II) complex showed rectangular, irregular crystals with an

average minute size of 67.2 nm. The image of FESEM analysis of the Cu (II) complex appeared in the form of heterogeneous spherical crystals, and the average particle size was 65.6. As noted from the results obtained through FESEM images shown in Fig 5. below, it is clear that all the complexes were within the nanoscale and that this feature made them can be used in several fields, including the field of medicine as a treatment against many types of cancers. The possibility of the ligand was studied. (HL) and its complexes inhibit colon and rectum cancer cells in our current study to see the possibility of using them as medicine, which we will explain later.

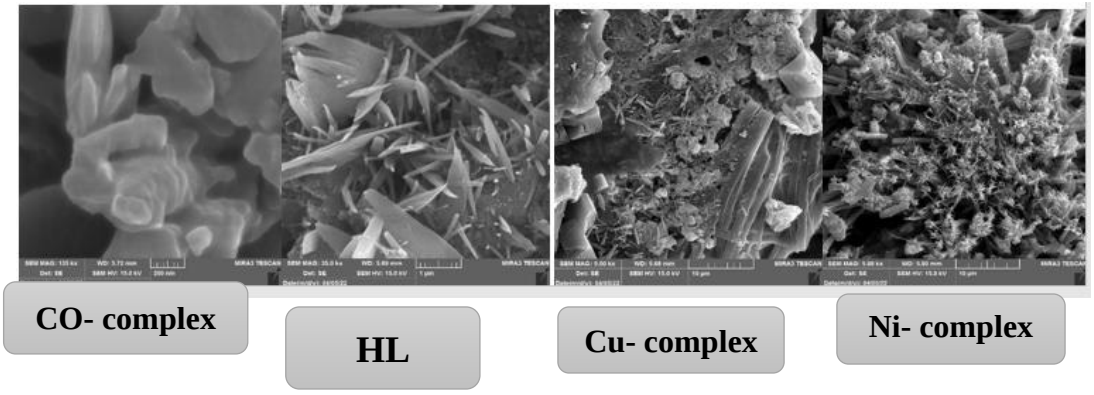

Figure 5. FE-SEM images of ligand (HL) and chelate complexes

X-ray diffraction study (XRD)

The ligand (HL) and its metal complexes in their solid-state were analyzed using X-ray diffraction within (angular range 2θ= 10°-80°) to know some structural properties, crystal structures, and crystal sizes. Micro strains and the density of dislocations were also calculated. density) to determine the extent of its purity and the defects in the crystal structure when converting the ligand into metal complexes There are some diffraction peaks for which a review occurs for many reasons, including the microstrain, such as the lack of the crystal lattice deformation and crystal cracking (Faulting) that occurs as a result of distortions that occur in the crystal, and the domain size of the crystal, and the Distribution of domain. The Debye-Scherer equation was also used to calculate the crystal size of ligand (HL) and their metal complexes, as follows(Shakir et al. 2015).

$$D = \frac{0.9\,\lambda}{\beta\cos\theta} \quad (1)$$

where D = average crystal size, k = the shape factor, which is usually about 0.9, λ = represents the wavelength of X-rays, and its value is CuKα = 1.54056 A°, β = total width half maximum height F.W.H.M, θ = is the angle of deviation. The following equation was also used to calculate the micro-compliance: -

$$\delta = 1/D^2 \quad (2)$$

Where δ represents the atomization density and D = the average crystal size. Through the X-ray spectra, apparent differences were observed in the previously mentioned data, such as crystal size, microplasticity, dissolution density, and the spacing between the crystalline levels of the ligand and its prepared metal complexes. Microstructure and the density of atomizations, so that the higher the crystal size, the lower the microplasticity and the less the density of the atomizations, thus reducing the defects of the crystal. In addition, we found that the ligand and its metal complexes have a grain size of less than 100 nm. They are within the nanoscale, and at the same time, these results reinforce our measurements of Previous Emission Field Scanning Electron Microscopy (FESEM) analyses. Table (5) and Figure (6) shows the diffraction angles, observed values, relative intensity, crystal size, crystal tension, widths of peaks at mid-strength, micro-compliance, and decay density for each of the ligands (HL) and its metal complexes: -

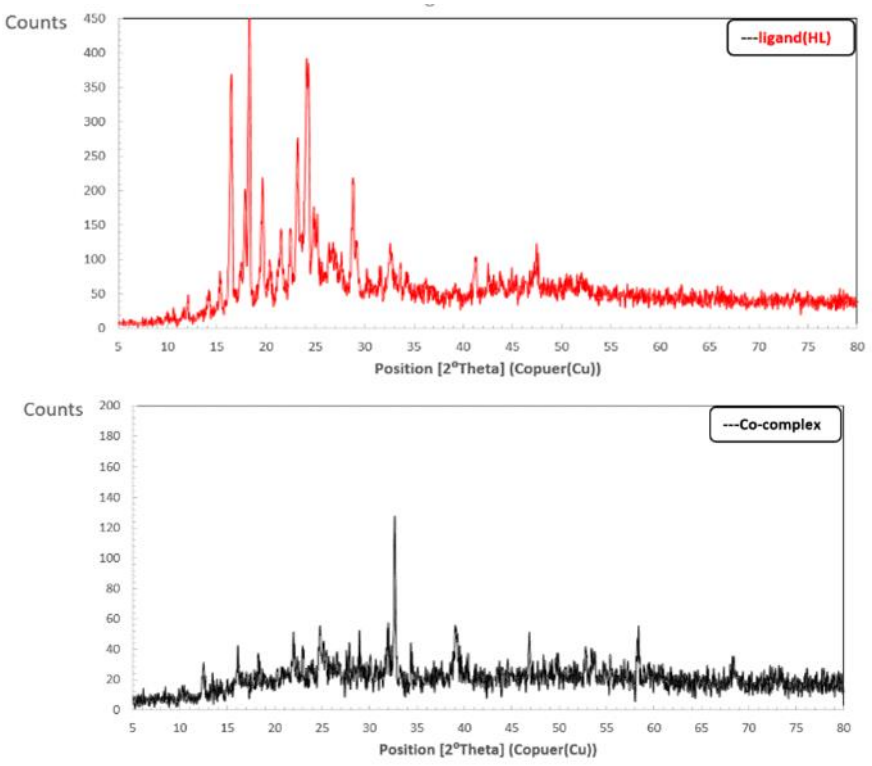

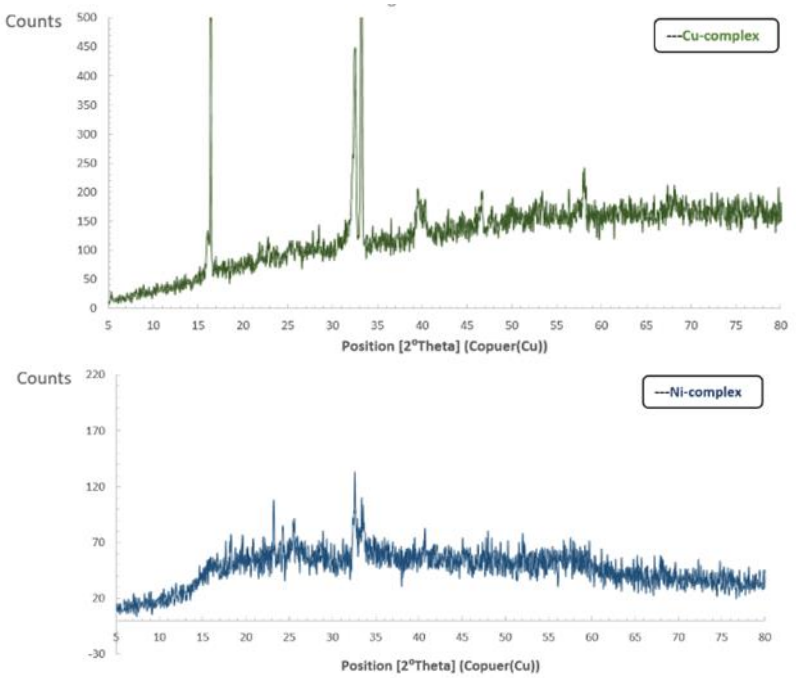

Figure 6. X-ray diffraction spectrum of ligand azo- Schiff base (HL) and its prepared metal complexes

Table 5
Diffraction angles, observed d values, relative intensity, crystal size, crystal tension, symptoms of peaks at mid-intensity, micro-compliance, and dissolution intensity of the ligand (HL) and its metal complex Compound

	No	$2\theta_{observed}$ (°)	d-observed (Å)	I/Io (%)	FWHM.	Crystallite size (nm)	Lattice strain	$\delta_D X10^{15}$ (lin m^{-2})
Ligand=HL	1	16.4687	5.38277	69.11	0.23616	50.1	0.0006	0.398
	2	19.6402	4.52015	28.6	0.23616	35.4	0.0059	0.797
	3	21.4975	4.13364	13.13	031488	26.3	0.0072	1.445
	4	24.2938	3.66382	63.07	0.15744	54.5	0.0031	0.336
	5	28.76639	3.10354	30.81	0.23616	36.0	0.00401	0.771
Co(III)-complex	1	12.4494	7.11267	19.47	0.3148	26.0	0.0126	1.479
	2	16.23174	5.46084	10.54	0.94464	8.6	0.0289	13.52
	3	24.82885	3.58607	18.41	0.47232	17.5	0.00935	3.322
	4	32.65451	2.74235	100	0.15744	55.6	0.00234	0.323
	5	39.11627	2.30293	30.95	0.47232	18.2	0.00580	3.018
	6	58.28061	1.5832	23.36	0.23616	39.9	0.00185	0.628
Ni(II)-complex	1	18.2128	4.87105	53.82	0.23616	35.3	0.00642	0.802
	2	23.18864	3.83587	82.33	0.23616	35.6	0.00502	0.789
	3	25.53313	3.48873	61.33	0.47232	17.5	0.00911	3.265
	4	32.4791	2.75675	100	0.31488	27.0	0.00472	1.371
Cu(II)-complex	1	16.37166	5.4149	67.1	0.11808	73.0	0.00357	0.187
	2	32.50108	2.75494	38.16	0.23616	36.3	0.00353	0.758

	3	33.18841	2.69944	100.00	0.15744	55.6	0.00230	0.323
	4	39.5068	2.28106	6.85	0.47232	18.2	0.00573	3.018
	5	46.53266	1.95171	4.95	0.47232	18.6	0.00479	2.890
	6	58.07046	1.58842	6.38	0.31488	19.6	0.00248	2.603

Antimicrobial activity

The antibacterial activity of the synthesized compounds was tested against two species of harmful bacteria: Staphylococcus aureus a gram-positive bacteria) and Escherichia coli (a gram-negative bacteria). Moreover, a Penicillium fungus class determines the inhibitory effect of Ligand and its complexes on their growth. The biological effects of ligand solutions and their metal complexes generated at a concentration of $1*10^{-3}$ M with bacteria and fungus were presented in Table (6) and the images in Figure (7).

Table 6
Effect of ligand (LH) and its metal complexes dissolved in DMSO solvent on two types of bacteria and one type of fungi

Compound	Staphylococcus	E. coli	Penicillium sp.
HL	+++	++	+++
Co(Ill)-Complex	+++	+	+++
Ni(ll)-Complex	++	++	++
Cu(ll)-Complex	++	++	+++

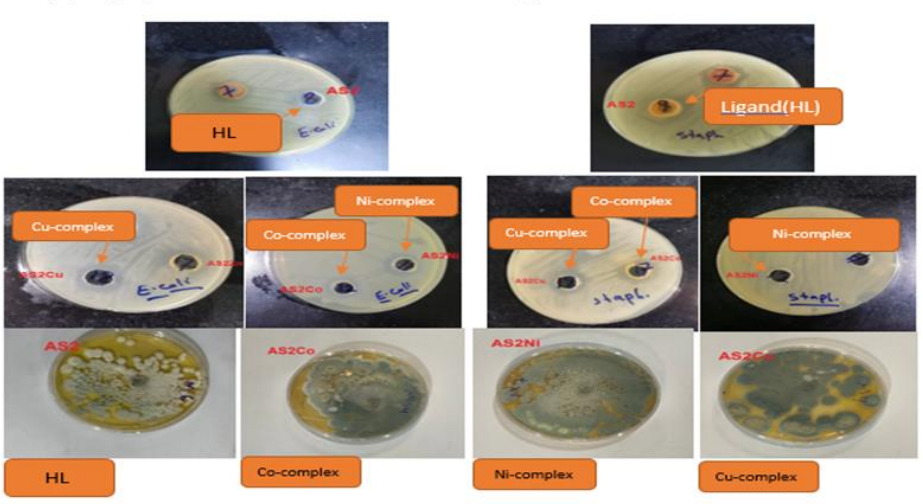

Figure 7. The biological effect of Ligand (HL) and its metal complexes

Anti-cancer effect (Cytotoxicity by use Assays (MTT)

This study included cell lines colorectal cancer cell line SW480 and standard cell line HUVEC for comparison. (MTT) to examine the vitality of all cells. The results

showed that the type of the prepared compound and its concentration are of great importance in determining the percentage of cytostatic. It depends mainly on concentrations and other factors, and this phenomenon is called dose-dependent, which many agreed upon of researchers(Sirivibulkovit et al. 2018).

Colorectal cancer cell line SW480
The effect of the Ligand (HL) on the growth process of colorectal cancer cells (SW480) and normal cells (HUVEC)

When studying the effect of Ligand (HL) on the growth process of colorectal cancer cell lines (SW480) and normal cells (HUVEC), the lowest percentage of cell growth inhibition appeared for colorectal cancer (SW480) and normal cells (HUVEC) at concentrations µg/ml 15.625 For both, while the highest inhibition rate was at 500 µg/ml for colorectal cancer cells (SW480) and normal cells (HUVEC) together, and healthy cells (HUVEC) were used for comparison to know the possibility of using it in the medical field as a drug. It was found that the percentage of the number of live cells remaining after the reaction with the Ligand (HL) ranged between (13.55646% - 97.5418 for the cells of the colorectal cancer cell line SW480, while the percentage of cells of the normal cell line (HUVEC) was between (35.2149% - 92.23347%). The best percentage of inhibition of the cell line of colorectal cancer (SW480) appeared at the concentration - 500 µg/ml 86.44%. In comparison, the percentage of inhibition of the cell line of the normal healthy cells (HUVEC) was 64.79%, which is an excellent result as its effect on cancer cells is greater. From its effect on healthy cells, this, in turn, also shows us the possibility of using the mentioned Ligand as a treatment for colorectal cancer. Table (7) and the following Figure (8) illustrate this. The Ligand (HL) reaction with the colorectal cancer cell line SW480. 250.6 µg/ml, while the half inhibitory concentration of normal HUVEC cells reached 253.2 µg/ml. The following figure (9) shows the relationship between the half inhibitory concentration (IC50) of the Ligand (HL) with cells of the colorectal cancer line (SW480) and cells of the normal cell line HUVEC.

Table 7
Comparison of the effect of azo-base compound (HL) on the cells of the colorectal cancer line SW480 with that of a normal cell line at the same concentration using MTT assay for 48 hours at 37°C

Con.(µg.mL^{-1})	ligand (HL)			
	SW480 line cells of Cancer		line cells HUVEC Normal	
	Mean	SD	Mean	SD
15.625	97.5418	4.609356	92.23347	7.280139
31.25	96.54139	6.44867	74.65054	9.835346
62.5	93.4775	7.720248	62.325	6.815347
125	69.57133	5.604497	58.235	7.635856
250	53.07685	7.599238	52.321	2.486821

500	13.55646	6.11997	35.2149	5.680729

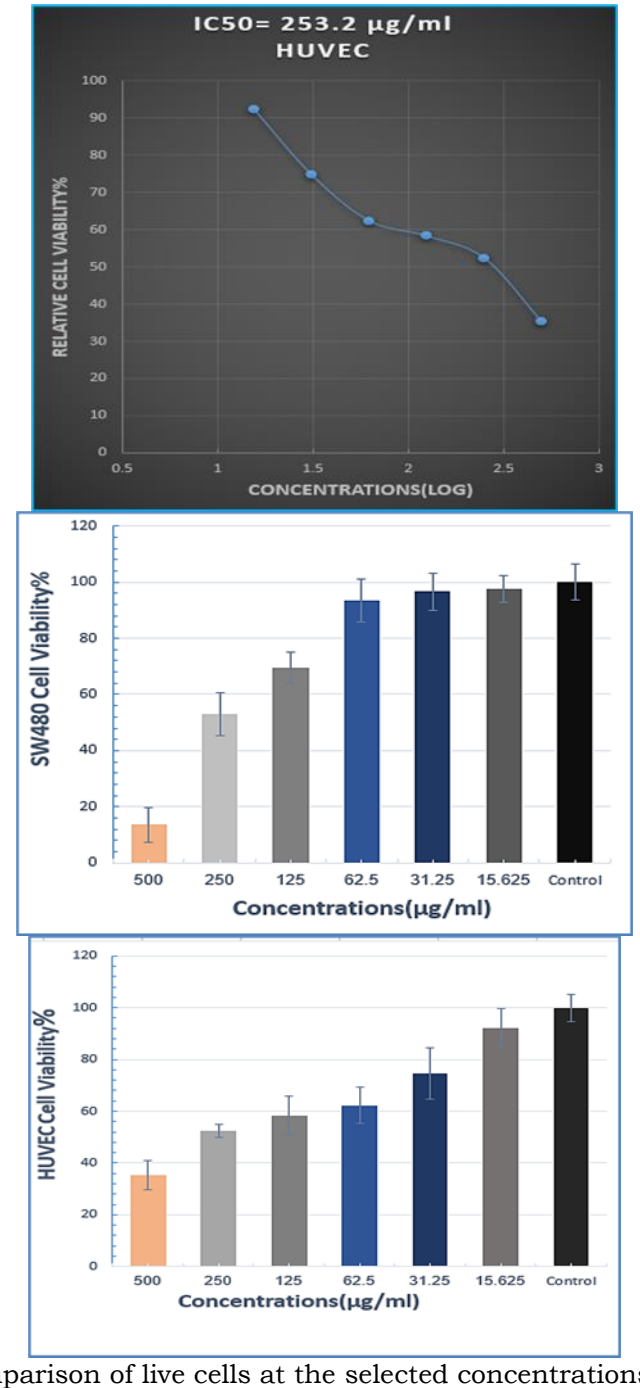

Figure 8. Comparison of live cells at the selected concentrations of cells of the colorectal cancer cell line SW480 and cells of the normal cell line HUVEC of the azo Ligand - Schiff base (HL)

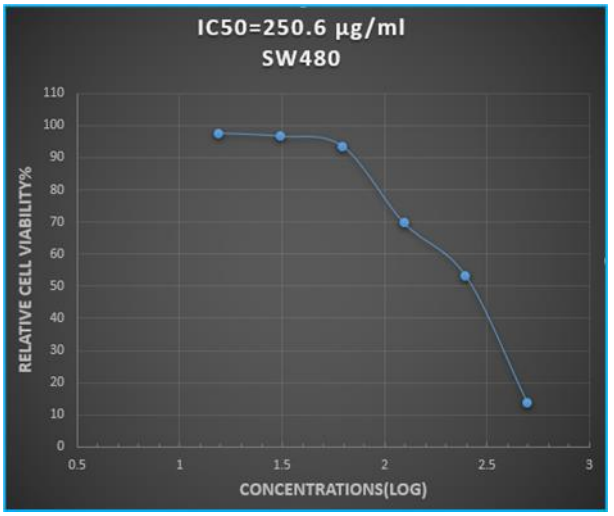

Figure 9. The relationship between the biological activity of SW480 colorectal cancer line cells and HUVEC normal cell line cells versus the concentration of the azo Ligand - Schiff base (HL)

Effect of nickel (II) complex with Ligand (HL) on the growth of SW480 colorectal cancer cells and normal cells (HUVEC)

The effect of nickel (II) complex $[Ni(HL)_2]Cl_2.H_2O$ on the growth process of colorectal cancer cell lines (SW480) and healthy cells (HUVEC) gave the lowest percentage of growth inhibition of colorectal cancer cell lines (SW480). At the concentration of 15.625 µg / ml and the same concentration for normal cells (HUVEC), the highest percentage of inhibition appeared at 500 µg / ml for colorectal cancer cells (SW480) and normal healthy cells (HUVEC). The obtained results showed that the percentage of the number of cells remaining after its interaction with the metallic complex of nickel (II), ranging between (9.5850% - 99.6571%) belonging to the cells of the colorectal cancer cell line (SW480), while the percentage of cells of the normal healthy cell line (HUVEC) ranged between (36.0056% - 99.7603%). The best percentage of inhibition of colorectal cancer cell line (SW480) at a concentration of 500 µg/ml was 90.42%. At the same time, the percentage of inhibition of cell lines of normal healthy cells (HUVEC) at the same concentration was 63.99%, as shown in Table (8) and Figure (10). The inhibitory concentration was also the Inhibition Concentration Fifty (IC50) halves when reacting the metallic complex of nickel (II) with the colorectal cancer cell line SW480. µg/ml 68.42 µg/ml, while the half inhibitory concentration of HUVEC normal cells was 154.6 µg/ml. The following figure (11) shows the relationship between the half inhibitory concentration (IC50) of the nickel complex (II) with the cells of the colorectal cancer line (SW480) and the cells of the normal cell line HUVEC.

Table 8
Comparison of the effect of nickel (II) complex with Ligand (H L) on cells of colorectal cancer line SW480 with that of normal cell line at the same concentration using MTT test for 48 hours at 37°C

Con.(µg.mL^{-1})	Ni (II)-complex			
	Cancer line cells of SW480		Normal line cells HUVEC	
	Mean	SD	Mean	SD
15.625	97.5418	4.609356	92.23347	7.280139
31.25	96.54139	6.44867	74.65054	9.835346
62.5	93.4775	7.720248	62.325	6.815347
125	69.57133	5.604497	58.235	7.635856
250	53.07685	7.599238	52.321	2.486821
500	13.55646	6.11997	35.2149	5.680729

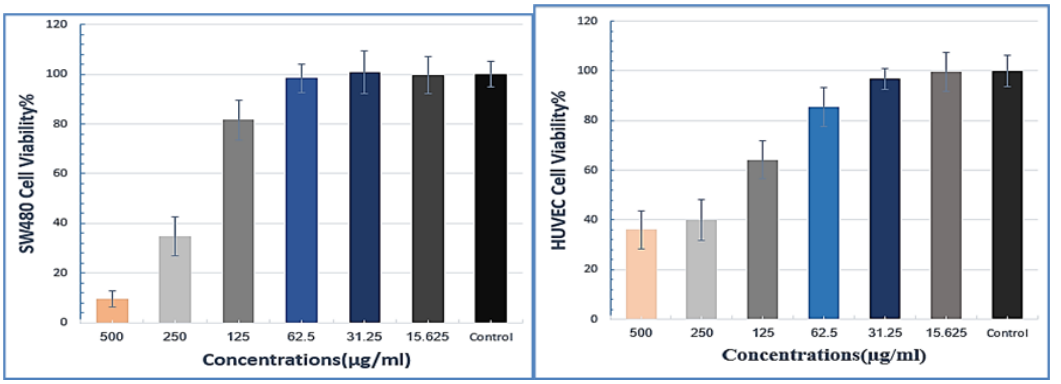

Figure 10. Comparison of live cells at the selected concentrations of cells of the colorectal cancer cell line SW480 and cells of the normal cell line of the nickel complex (II) with a ligand (HL)

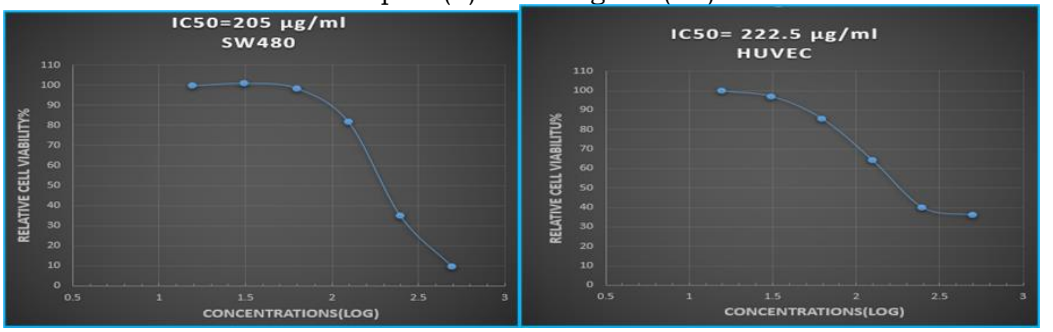

Figure 11. The relationship between the biological activity of the colorectal cancer line SW480 and cells of the normal cell line HUVEC versus the concentration of nickel (II) complex with (HL) ligand

Antioxidants

The results of the antioxidant analyze showed that the azo Ligand - Schiff base (HL) with its metal complexes under study, namely cobalt (III) and nickel (II), in comparison with ascorbic acid, possess antioxidant properties. In contrast, it was found that the least inhibition of free radicals in relation to the concentrations of each From the Ligand (HL) and its complexes. At the lowest concentration of 19.53125 mg/ml it is (12.1227%) (37.6554%) (30.1784%) respectively. It was found that the highest rate of inhibition of free radicals was at the concentrations of each of the ligands. Its complexes are cobalt (III) and nickel (II), with the same concentrations being (89.3247%) (74.1342%) (77.4243%), respectively. Figures (12) to (17) show the results obtained(Sirivibulkovit et al. 2018).

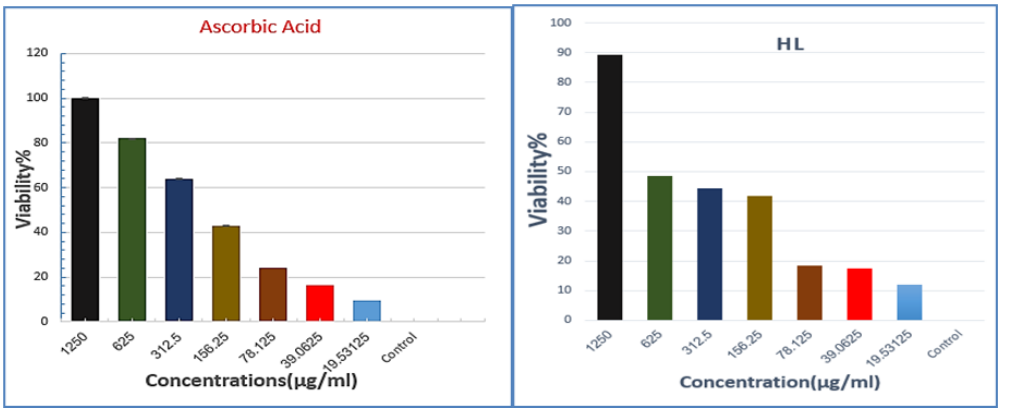

Figure 12. Percentage of inhibition compared to ascorbic acid with Ligand (HL)

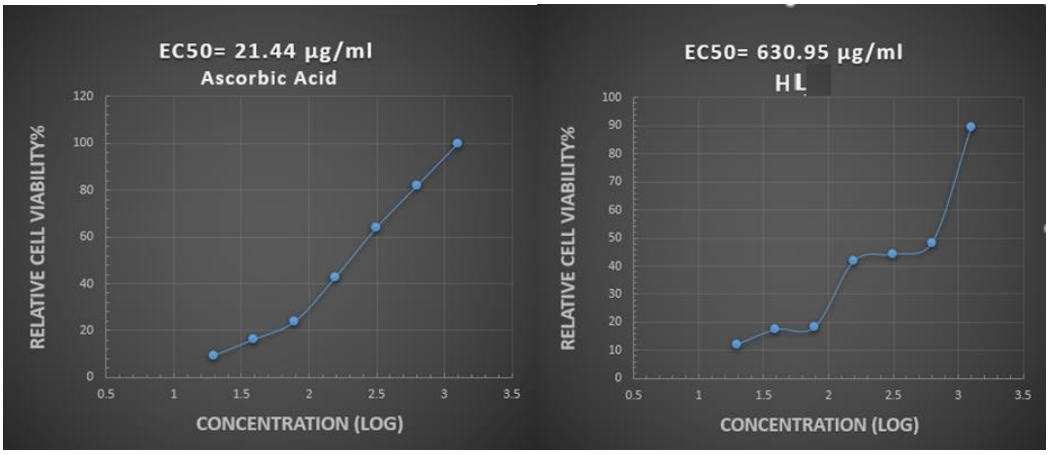

Figure 13. The relationship between the inhibiting activity of free radicals versus the concentration of ligand (HL) in comparison with ascorbic acid

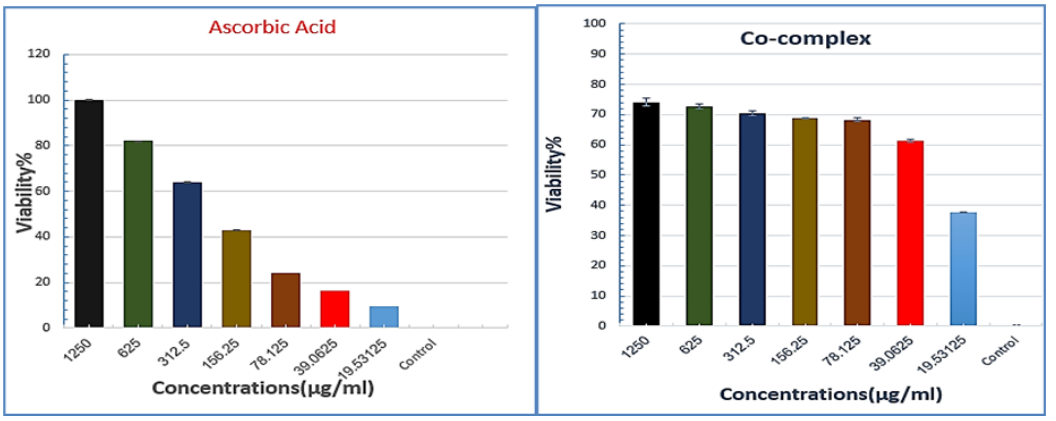

Figure 14. Percentage of inhibition compared to ascorbic acid for the complex of cobalt (III) with Ligand (HL)

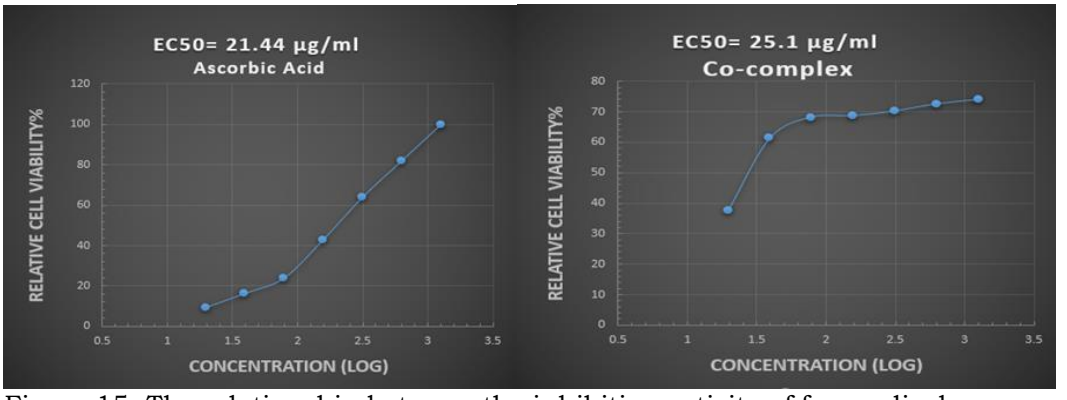

Figure 15. The relationship between the inhibiting activity of free radicals versus the concentration of cobalt (III) complex with Ligand (HL) compared to ascorbic acid

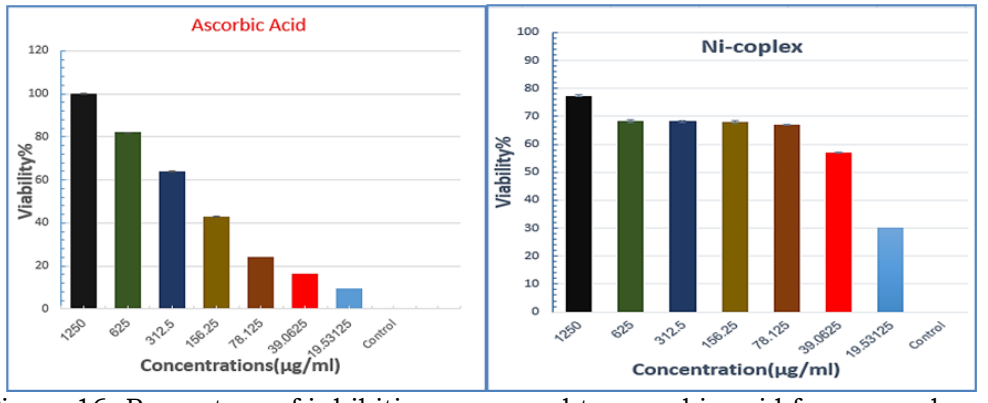

Figure 16. Percentage of inhibition compared to ascorbic acid for a complex of nickel (II) with Ligand (HL)

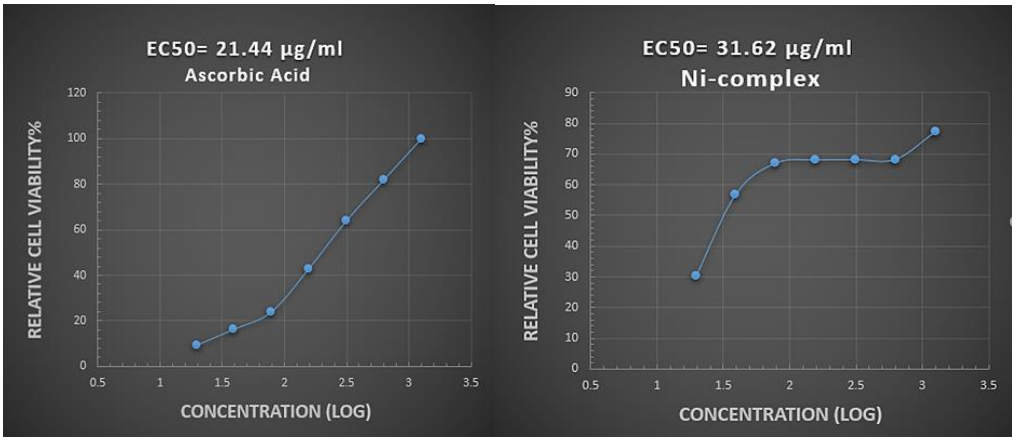

Figure 17. The relationship between the inhibiting activity of free radicals versus the concentration of nickel (II) complex with Ligand (HL) in comparison with ascorbic acid

Conclusion

The Ligand derived from benzothiazole has been prepared, and the complexes of this Ligand are the divalent cobalt, nickel, and copper complexes. They were identified by conducting several analyses, such as ultraviolet and infrared spectroscopy, 1HNMR, magnetic sensitivity, XRD, FE-SEM techniques, and molar conduction. It was proved that the complexes have different structures and shapes. The Ligand is coordinated with the metal from three binding sites: the nitrogen of the azo group, the nitrogen of the thiazole ring, and the oxygen of the hydroxyl group after losing its proton. The molar conductivity results revealed a chloride ion outside the coordination domain. FE-SEM images of the prepared metal complexes demonstrated that the Ligand and its complexes were nanoparticles that could be used for cancer treatment. Biological activity and toxicity of the Ligand and its complexes were performed.

References

Al-Adely KJ (2012) Synthesis and spectrophotometric studies of some transition metal complexes with new azo dye 2-[2-(6-methoxy benzothiazo-lyl) azo]-4-nitro phenol. Asian J Chem 24:5597-5601

Al-Adilee KJ, Hesson H (2015) Synthesis, identification, structural, studies and biological activity of some transition metal complexes with novel heterocyclic azo-Schiff base ligand derived from benzimidazole. J Chem Pharm Res 7(8):89-103

Al-adilee KJ, Hessoon H Synthesis, Spectral properties and anticancer studies of novel hetrocyclic azo dye ligand derived from 2-Amino-5-methyl thiazole with some transition metal complexes. In: Journal of Physics: Conference Series, 2019. vol 1234. IOP Publishing, p 012094

Al-Adilee KJ, Shaimaa A (2017) Synthesis and Spectral Properties Studies of Novel Hetrocyclic Mono Azo dye Derived from Thiazole and Pyridine with Some Transition Complexes. OJC 33(4):1-14

Alshamsi HA, Al Bedairy MA, Alwan SH Visible light assisted photocatalytic degradation of Rhodamine B dye on CdSe-ZnO nanocomposite: Characterization and kinetic studies. In: IOP Conference Series: Earth and Environmental Science, 2021. vol 722. IOP Publishing, p 012005

Bai S, Hu J, Li D, Luo R, Chen A, Liu CC (2011) Quantum-sized ZnO nanoparticles: synthesis, characterization and sensing properties for NO 2. Journal of Materials Chemistry 21(33):12288-12294

Benkhaya S, M'rabet S, El Harfi A (2020) Classifications, properties, recent synthesis and applications of azo dyes. Heliyon 6(1):e03271

El-Ghamry HA, Fathalla SK, Gaber M (2018) Synthesis, structural characterization and molecular modelling of bidentate azo dye metal complexes: DNA interaction to antimicrobial and anticancer activities. Applied Organometallic Chemistry 32(3):e4136

Harisha S, Keshavayya J, Swamy BK, Viswanath C (2017) Synthesis, characterization and electrochemical studies of azo dyes derived from barbituric acid. Dyes and Pigments 136:742-753

Jaber SA, Kyhoiesh HA, Jawad SH Synthesis, characterization and biological activity studies of cadmium (II) complex derived from azo ligand 2-[2\-(5-bromo Thiazolyl) azo]-5-dimethyl amino benzoic acid. In: Journal of Physics: Conference Series, 2021. vol 1818. IOP Publishing, p 012013

Khalid J (2018) Al-Adilee and sudad A. Jaber. Asian J chem 30(7):1537-1545

Kyhoiesh HAK, Al-Adilee KJ (2021) Synthesis, spectral characterization, antimicrobial evaluation studies and cytotoxic activity of some transition metal complexes with tridentate (N, N, O) donor azo dye ligand. Results in Chemistry 3:100245

Kyhoiesh HAK, Al-Adilee KJ (2022) Synthesis, spectral characterization and biological activities of Ag (I), Pt (IV) and Au (III) complexes with novel azo dye ligand (N, N, O) derived from 2-amino-6-methoxy benzothiazole. Chemical Papers 76(5):2777-2810

Maliyappa M, Keshavayya J, Mallikarjuna N, et al. (2019) Synthesis, characterization, pharmacological and computational studies of 4, 5, 6, 7-tetrahydro-1, 3-benzothiazole incorporated azo dyes. Journal of Molecular Structure 1179:630-641

Mallikarjuna N, Keshavayya J (2020) Synthesis, spectroscopic characterization and pharmacological studies on novel sulfamethaxazole based azo dyes. Journal of King Saud University-Science 32(1):251-259

Mohammadi A, Khalili B, Tahavor M (2015) Novel push–pull heterocyclic azo disperse dyes containing piperazine moiety: Synthesis, spectral properties, antioxidant activity and dyeing performance on polyester fibers. Spectrochimica Acta Part A: Molecular and Biomolecular Spectroscopy 150:799-805

Prajapati NP, Vekariya RH, Borad MA, Patel HD (2014) Recent advances in the synthesis of 2-substituted benzothiazoles: a review. Rsc Advances 4(104):60176-60208

Prakash S, Somiya G, Elavarasan N, et al. (2021) Synthesis and characterization of novel bioactive azo compounds fused with benzothiazole and their versatile biological applications. Journal of Molecular Structure 1224:129016

Shakir M, Hanif S, Sherwani MA, Mohammad O, Al-Resayes SI (2015) Pharmacologically significant complexes of Mn (II), Co (II), Ni (II), Cu (II) and Zn (II) of novel Schiff base ligand,(E)-N-(furan-2-yl methylene) quinolin-8-amine:

synthesis, spectral, XRD, SEM, antimicrobial, antioxidant and in vitro cytotoxic studies. Journal of Molecular Structure 1092:143-159

Sirivibulkovit K, Nouanthavong S, Sameenoi Y (2018) based DPPH assay for antioxidant activity analysis. Analytical sciences 34(7):795-800

Waheeb AS, Kyhoiesh HAK, Salman AW, Al-Adilee KJ, Kadhim MM (2022) Metal complexes of a new azo ligand 2-[2′-(5-nitrothiazolyl) azo]-4-methoxyphenol (NTAMP): Synthesis, spectral characterization, and theoretical calculation. Inorganic Chemistry Communications 138:109267

Yadav P, Devprakash D, Senthilkumar G (2011) Benzothiazole: different methods of synthesis and diverse biological activities. ChemInform 42(40):no-no